

# Catalytically active nanostructures derived from self-assembled block copolymer templates for rationally synthesizing single-walled carbon nanotubes and understanding the growth mechanism

J. Lu<sup>\*</sup>, Q. Fu<sup>\*\*</sup>, C.G. Lu<sup>\*\*</sup>, J. Liu<sup>\*\*</sup>

<sup>\*</sup>School of Engineering, University of California at Merced, Merced, CA 95344

<sup>\*\*</sup>Chemistry Department, Duke University, Durham, NC 27708

## ABSTRACT

Employing self-assembled catalyst-containing block copolymer templates, we have successfully generated a variety of highly ordered and uniform-sized catalytically active transition metal nanostructures. These catalyst-containing nanostructures have been used to produce high-quality and single-walled carbon nanotubes (CNTs) with narrow size distribution. By tailoring the chain length of each block, we have rationally adjusted the size and spacing of catalyst nanostructures and subsequently the density and diameter of CNTs. Combining this bottom-up self-assembly technique with conventional top-down microfabrication processing, lithographically selective growth of CNTs on surfaces and CNTs suspended across trenches over a large surface area has been obtained. This facile and highly manufacturable method has enabled the investigation of the fundamental CNT growth mechanism. The interplay between catalyst and local environment, such as carbon gas concentration and substrate on CNT growth will be presented.

**Keywords:** carbon nanotube synthesis, block copolymer template, self-assembly, catalyst, growth mechanism

## 1 INTRODUCTION

Single-walled CNTs which can be viewed as a single sheet of graphene rolled up into a nanocylinder, are chemically inert and mechanically robust. Their remarkable electron transport and unique optical properties as well as excellent adsorption capability have sprouted burgeoning efforts to develop devices that utilize these properties. The CNT-based field-effect transistor has demonstrated near ballistic electron transport behavior and CNTs have been explored for applications in biosensing, bioimaging and drug delivery.[1-4] However, these efforts have achieved limited commercial success to date largely due to the lack of precise control of size and placement of CNTs. Developing robust synthesis methods to generate defect-free CNTs with predictable and consistent physical properties is the key to bring their highly touted potential into fruition.

Chemical vapor deposition has gained popularity as a carbon nanotube fabrication method in which CNTs are grown selectively on catalytic sites. It has become the standard technique for synthesizing single-walled and

multi-walled CNTs for substrate-based applications. It has been well acknowledged that the catalyst system determines the characteristics of CNTs. Therefore, a method for producing well-defined catalyst nanostructures with controlled size and spacing is paramount for achieving controllable synthesis of CNTs. We have developed a methodology using morphologies produced by self-assembling block copolymers to generate uniform and well-ordered catalyst-containing nanostructures with tunable size, spacing and composition at predefined locations. The ability of controlling catalyst-containing nanostructures at the nano-, micro- and macro-scales simultaneously has greatly enhanced the manufacturability of CNTs. CNTs with adjustable diameter and density at predetermined locations have been synthesized. These uniform and reproducible catalyst substrates have also facilitated the systematic investigation of the growth mechanism. We have found that for a given catalyst system, there is a corresponding unique growth condition for generating defect-free CNTs with a minimum amount of deposited amorphous carbon. The ability of catalyst to initiate CNT growth highly depends on the local environment such as the catalyst support and carbon gas concentration. Understanding the interplay between CNT growth conditions such as local carbon stock concentration and catalyst will shed light on the CNT growth mechanism. This in turn will help to develop a rational CNT synthesis method.

## 2 BLOCK COPOLYMER TEMPLATES

A block copolymer consists of two or more polymer segments joined together by covalent bonds. Due to the inherent immiscibility of segments, they can be self-assembled into well-ordered morphology ranging from several to hundreds of nanometers. The morphology varies from spheres to cylinders to lamellae with increase of the volume fraction of each component. These self-assembled morphologies are emerging as elegant scaffolds and templates for fabricating nanoscaled material.[5-6] To utilize these self-assembled morphologies as templates for creating catalyst-containing nanostructures, catalyst species need to be selectively incorporated onto one of the blocks.

### 2.1 Catalyst-containing block copolymers

Carbon has finite solubility in many transition metals such as iron. Over saturation of carbon atoms results in the precipitation of carbon and the formation of tubular carbon solid with sp<sup>2</sup> structure. Iron, nickel and cobalt have been widely used for the synthesis of CNTs. There are two basic methods of attaching these catalytically active metals onto polymers. One involves binding metallic species to a monomer prior to the polymerization. The other involves the incorporation of metals onto a pre-existing block copolymer.

In the first method, an appropriate metal-containing monomer is chosen to be polymerized into metal-containing polymer. For example, vinylferrocene, an iron-containing monomer, can be synthesized by free radical polymerization to form the iron-containing polymer. Using anionic living polymerization of styrene followed by the ring-opening polymerization of silaferrocenophane, polystyrene-*b*-polyferrocenylethylmethylsilane polymers has been synthesized (denoted PS-*b*-PFEMS).[6-7] Figure 1e shows the chemical structure of PS-*b*-PFEMS.

Since for many reaction paths the presence of metal may terminate the polymerization, only a few transition metal coordinated monomers undergo polymerization, especially for using living anionic polymerization for synthesizing metal-containing block copolymers. A more convenient way to form metal-containing block copolymer is to bind metal precursors onto pre-formed block copolymers via coordination bonds or ionic bonds. Figure 1f shows an example of iron attached onto a segment of a block copolymer via complexation, in which the pyridine group forms a coordination bond with iron by donating the lone pair of electrons on nitrogen to the empty d-orbitals of iron.

## 2.2 Catalyst-containing nanostructures

PFEMS is less polar than PS and the glass transition temperatures for PFEMS and PS are 15 °C and 95 °C respectively. Due to the chemical and physical dissimilarity between these two blocks, self-assembled morphologies can be attained in a thin film form on a properly treated surface. Figure 1a is a height image of a PS-*b*-PFEMS thin film acquired by atomic force microscopy (AFM). After organic components are removed by pyrolysis, close-packed iron-containing posts have been formed.

Polystyrene-*b*-poly(2-vinyl pyridine) (denoted PS-*b*-P2VP hereafter) readily incorporates transition metal onto the P2VP segment. Metal-bearing P2VP segment is very polar and as a result the metal-modified block copolymer can spontaneously self-organized in a nonpolar solvent such as toluene to form micelles where the shell of a micelle is PS while the core is comprised of metal-complexed P2VP. A monolayer of highly-ordered surface micelles can be formed by spin-coating as illustrated by the AFM height image in Figure 1c. The resultant nanoparticles after UV-ozonation is displayed in Figure 1d.

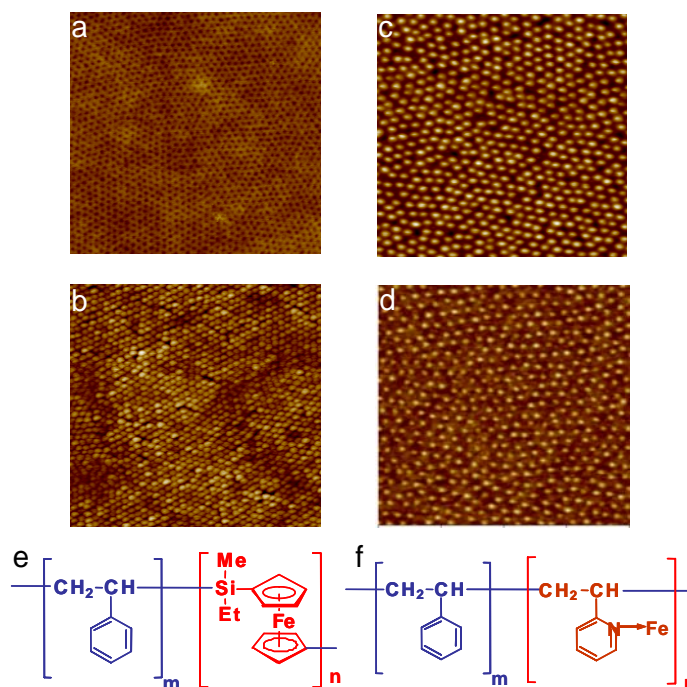


Figure 1 AFM height image of PS<sub>263</sub>-*b*-PFEMS<sub>44</sub> film, as deposited (a) and after pyrolysis (b); Iron complexed PS<sub>405</sub>-*b*-P2VP<sub>77</sub> as deposited (c) and after UV ozonation (d); Chemical structure of PS-*b*-PFEMS (e); Chemical structure of PS-*b*-P2VP (f). All AFM images are 1 μm by 1 μm scan, 10 nm in height.

Using this technique, we have been able to generate nickel and cobalt nanoparticles with uniform size and spacing.[8] By attaching more than one metal species, bimetallic metal such as iron/nickel, iron/molybdenum and cobalt/ molybdenum have also been generated. Figure 2 display a set of AFM images and their associated X-ray photoelectron spectra (XPS) of surfaces prepared from a solution of PS-*b*-P2VP with an iron salt and a mixture of iron and nickel salts. According to XPS analysis, the nanoparticles derived from the iron complexed block copolymer solution has only one peak in the binding energy region corresponding to Fe2p<sub>3/2</sub> at 711 eV while the sample prepared from a mixture of iron and nickel salt has peaks both at 711 eV (generated by Fe2p<sub>3/2</sub>) and 856.4 eV (produced by Ni 2p<sub>3/2</sub>). The AFM images confirm that well-ordered bimetallic nanoparticles have been generated by this approach. By adjusting the molar ratio, the composition of bimetallic nanoparticles can be tuned.

The table in Figure 3 summarizes the spacing of nanoparticles generated from different block copolymer systems. A mathematical fit of the data yield a scaling relationship of interparticle separation,  $d \sim 2 \times N_{ps}^{0.59}$  ( $N_{ps}$  is the number of repeat units of polystyrene) as shown in Figure 3a. This result indicates that when the PS chain is relatively long, the configuration of PS chains on the surface is the same as in a good solvent. The distance

between nanoparticles is solely controlled by  $N_{ps}$ . Therefore by using polymer systems with different  $N_{ps}$ , the interparticle spacing can be tailored accordingly.

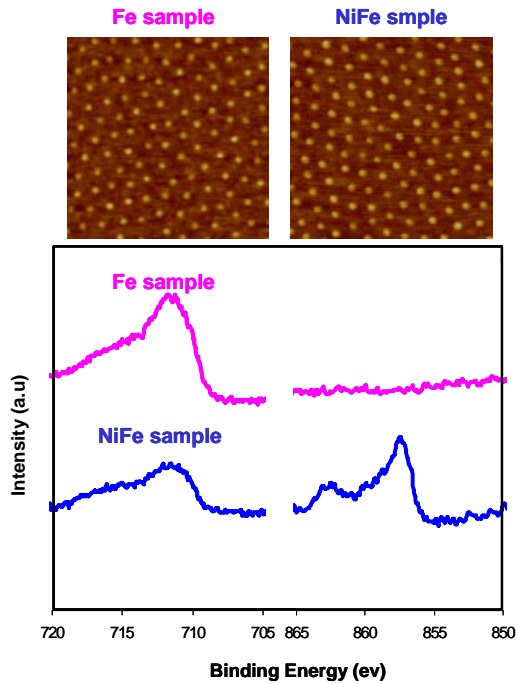


Figure 2. (a) AFM height images of nanoparticles prepared from PS<sub>1814</sub>-b-P2VP<sub>314</sub> (0.5 by 0.5  $\mu\text{m}$  scan size, 10 nm in height); (b) corresponding XPS spectra.

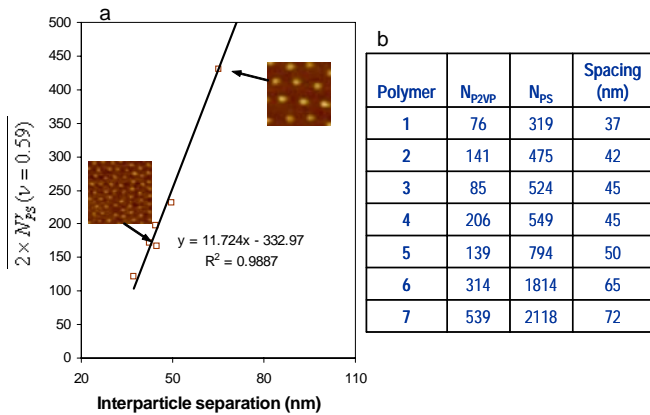


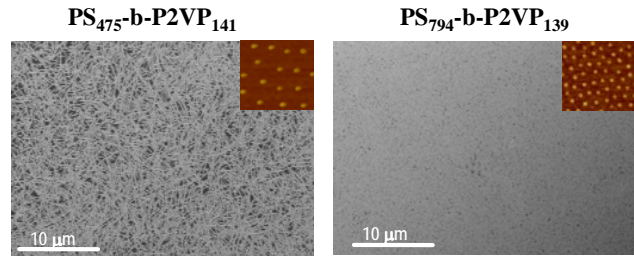
Figure 3. (a)  $2 \times N_{PS}^{0.59}$  vs. interparticle spacing, (b) Summary of the interparticle spacing of iron nanoparticles.

### 3 CARBON NANOTUBE SYNTHESIS

#### 3.1 Diameter and density controlled growth

All the aforementioned catalytically active nanostructures have been used to produce single-walled CNTs with uniform density and tight diameter distribution.[8-9] Figure 4 describes an example showing that highly ordered cobalt nanoparticles with an average

diameter of 2.2 nm and 4.0 nm have been derived from PS<sub>475</sub>-b-P2VP<sub>141</sub> and PS<sub>794</sub>-b-PVP<sub>139</sub> respectively. Smaller and denser cobalt nanoparticles produced from PS<sub>475</sub>-b-P2VP<sub>141</sub> result in a highly dense CNT mat as shown by the SEM images in Figure 4. The summary of AFM height analysis listed in the table displayed in the Figure 4 indicates that smaller catalyst nanoparticles produce smaller diameter CNTs. Using 2.2 nm iron nanoparticles, CNTs have an average diameter of 1.1 nm. The average CNT diameter increases to 1.7 nm when 3.8 nm nanoparticles are used. Therefore the block copolymer template approach provides a rational method for adjusting the diameter and density of CNTs by tailoring the block lengths.



	nanoparticle size (nm)	CNT diameter (nm)	G/D (nm)
PS <sub>475</sub> -b-P2VP <sub>141</sub>	2.2 ( $\pm 0.1$ )	1.1( $\pm 0.4$ )	9
PS <sub>794</sub> -b-P2VP <sub>139</sub>	3.8 ( $\pm 0.2$ )	1.7( $\pm 0.5$ )	16

Figure 4. SEM images of CNT mats; Insets are AFM height images of cobalt nanoparticles. (1 by 1  $\mu\text{m}$  scan size, 10 nm in height); the table summarizes cobalt nanoparticle size, spacing and corresponding CNT diameter obtained from AFM height analysis and Raman analysis results of CNTs.

#### 3.2 Patterned growth

Both a self-assembled PS-b-PFEMS thin film and monolayer of surface micelles of metal-complexed polystyrene-b-poly(2-vinylpyridine) are fully compatible with conventional novolac-based photoresists. Using top-down microfabrication processing, ordered arrays of catalyst-containing nanostructures have been generated. Spatially selective growth of suspended single-walled carbon nanotubes across trenches and on surfaces over a large surface area has been achieved as displayed in Figure 5.

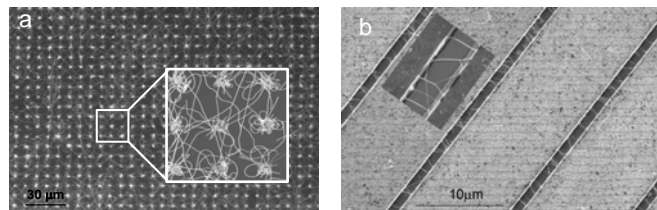


Figure 5. SEM images of patterned growth of CNTs on a surface (a) and across trenches (b).

## 4 CNT GROWTH MECHANISM

### 4.1 Catalyst support

We examined the role of catalyst support on CNT growth. In this study, we used iron nanoparticles derived from iron complexed PS-*b*-P2VP. The SEM images of CNTs displayed in Figure 6, elucidate that the surface on which catalyst nanoparticles are placed have a great influence on the overall growth of CNTs. Smaller diameter and longer CNTs with low defect density have been produced using a thermally grown silicon oxide surface whereas no growth was observed using the same nanoparticles on a silicon nitride support. This result indicates the importance of understanding the role of catalyst support on CNT growth.

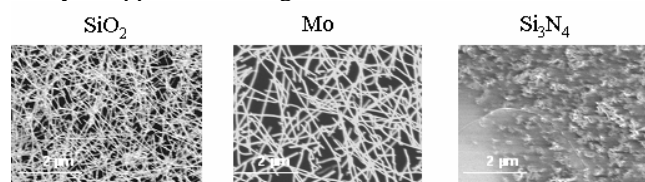


Figure 6. SEM images of CNTs grown on different surfaces

### 4.2 Catalyst size and carbon stock feed rate

We have demonstrated that using the same growth condition but employing catalyst nanostructures with different size, the amount of amorphous carbon and defect varies greatly. In the Raman spectra of CNTs, the G band represents the tangential vibration of carbon atoms in the  $sp^2$  arrangement in CNTs while the D band near  $1350\text{ cm}^{-1}$  is activated by defects. Thus the ratio of G to D can be used to determine the purity level of CNTs. G/D listed in the table in Figure 4 shows that higher purity CNTs are obtained from larger catalyst nanoparticles. This result implies that this specific growth condition is favorable for synthesizing higher quality CNTs using relatively larger catalyst nanoparticles. This finding further stresses that obtaining uniformly sized catalyst nanoparticle is essential for producing defect-free CNTs.

We also observed that the concentration of carbon stock or the carbon gas feeding rate also affects the growth yield dramatically. Figure 7 contain a set of SEM images of CNTs synthesized under different ethanol concentration. As can be seen, there is an optimal concentration for achieving high growth yield.

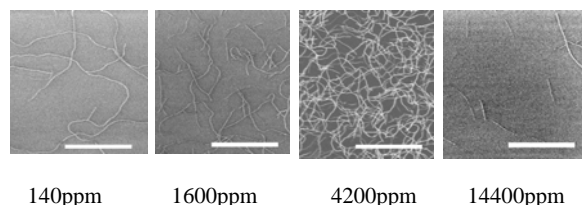


Figure 7. SEM images of CNT results as a function of ethanol concentration

## 5 ACKNOWLEDGEMENT

We would like to thank David Rider, Ian Manners and Mitchell Winnik at the University of Toronto for providing the PS-PFEMS samples and many valuable discussions.

## REFERENCES

- [1] Z. Liu, W. Cai, L. He, N. Nakayama, K. Chen, X. Sun, X. Chen, H. Dai, "In vivo biodistribution and highly efficient tumour targeting of carbon nanotubes in mice", *Nature Nanotechnology*, 2, 47, 2007.
- [2] H. Dai, A. Javey, E. Pop, D. Mann, Y. Lu. "Electrical Transport Properties and Field-Effect Transistors of Carbon Nanotubes", *NANO: Brief Reports and Reviews*, 1(1), 1, 2006.
- [3] G. Z. Yue, Q. Qiu, Bo Gao, Y. Cheng, J. Zhang, H. Shimoda, S. Chang, J. P. Lu, O. Zhou, "Generation of continuous and pulsed diagnostic imaging x-ray radiation using a carbon-nanotube-based field-emission cathode", *Phys. Lett.*, 81(2), 2002.
- [4] G. Gruner, "Carbon nanotube transistors for biosensing applications", *Anal. Bioanal. Chem.*, 384, 322, 2006.
- [5] M. P. Stoykovich, P. F. Nealey, "Block copolymer and conventional lithography" *MRS bulletin*, 9(9), 20, 2006.
- [6] D. A. Rider, K. A. Cavicchi, K. N. Power-Billard, T. P. Russell, I. Manners, *Macromolecules*, "Diblock Copolymers with Amorphous Atactic Polyferrocenylsilane Blocks: Synthesis, Characterization, and Self-Assembly of Polystyrene-*block*-poly(ferrocenylethylmethyl silane) in the Bulk State" 38(2), 6931, 2005
- [7] K. Temple, J.A. Masse, Z. Chen, N. Vaidya, A. Berenbaum, M.D. Foster, I. Manners, "Living Anionic Ring-Opening Polymerization of Unsymmetrically Substituted Silicon-Bridged [1]Ferrocenophanes: A Route to Organometallic Block Copolymers with Amorphous Polyferrocenylsilane Blocks", *J. Inorg. Organomet. Polym.*, 189, 9, 1999;
- [8] J. Lu, T. Kopley, G. Giralomi, Q. Cheng, J. Liu, E. Gulari, "Fabrication of ordered catalyst nanoparticles for controllable synthesis of carbon nanotubes" , *J. Phys. Chem. B*. 110(13), 6655, 2006.
- [9] J. Lu, T. Kopley, N. Moll, D. Roitman, D. Chamberlin, Q. Fu, J. Liu, T. Russell, D. Rider, I. Manners, M. Winnik, "High-quality single-walled carbon nanotubes with small diameter, controlled density, and ordered locations using a polyferrocenylsilane block copolymer catalyst precursor", *Chem. Mater.* 17, 2227, 2005